

## HYDRAULIC FRACTURING MICROSEISMIC FIRST ARRIVAL PICKING METHOD BASED ON NON-SUBSAMPLED SHEARLET TRANSFORM AND HIGHER-ORDER-STATISTICS

GUANQUN SHENG<sup>1,2</sup>, XINGONG TANG<sup>3,1</sup>, KAI XIE<sup>2</sup> and JIE XIONG<sup>2</sup>

<sup>1</sup> Key Laboratory of Exploration Technologies for Oil and Gas Resources (Yangtze University), Wuhan 430100, P.R. China.

<sup>2</sup> National Demonstration Center for Experimental Electrical and Electronic Education, Yangtze University, Jingzhou, Hubei 434000, P.R. China.  
Electronics and Information School, Yangtze University, Jingzhou, Hubei 434000, P.R. China.

<sup>3</sup> College of Geophysics and Petroleum Resources, Wuhan 430100, P.R. China

### ABSTRACT

Sheng, G.Q., Tang, X.G., Xie, K. and Xiong, J., 2019. Hydraulic fracturing microseismic first arrival picking method based on non-subsampled shearlet transform and higher-order-statistics. *Journal of Seismic Exploration*, 28: 593-618.

Fast and accurate first arrival picking is the key issue of microseismic data processing. Traditionally manual picking methods will take a lot of time and reduce the data processing efficiency, so it is difficult to meet the demand of real-time data processing for microseismic monitoring. In this paper, we proposed the S-S/L\_K (Shearlet-Short time window/Long time window-Kurtosis) algorithm which combined the shearlet multiscale decomposition with higher-order-statistics (HOS). This algorithm not only keeps the advantage of non-subsampled shearlet transform in multiscale analysis, but also maintain strengths of HOS in signal abnormalities detection and Gaussian noise suppressing. The forward records and real data tests show that compared with the PAI-S/K and the STA/LTA algorithm, the proposed method can overcome the influence of noise on the P-phase picking accuracy and obtain a reliable P-phase result for microseismic monitoring.

KEY WORDS: microseismic monitoring, non-subsampled shearlet transform, higher-order-statistics, first arrival picking.

## INTRODUCTION

Microseismic monitoring technology is to detect the underground state by observing and analyzing microseismic monitoring data produced by hydraulic fracturing, which is of great significance to the high production for oilfield development (Duncan and Eisner, 2010; Dong et al., 2016; Maxwell et al., 2010).

The effective signal energy of microseismic monitoring data is essentially weak and even completely submerged by the noise. However, satisfactory results cannot be easily obtained when conventional seismic data processing methods are applied directly, which will consequently affect the microseismic monitoring quality and precision (Gibbons and Ringdal, 2006; Karamzadeh et al., 2013). Therefore, exploring an appropriate method to identify weak effective signals is crucial to microseismic data processing and interpretation.

Fast and precise first arrival picking is the key issue of microseismic data processing, source location, source mechanism and fracture inversion (Maeda, 1985; Gou et al., 2011; Hafez et al., 2013; Alvarez et al., 2013). Nowadays, many scholars and experts have made a lot of research and progress. STA/LTA (Short-Term Average to Long-Term Average) has been proposed by Allen (1978). After that, this means has been widely applied to pick arrivals in many cases. Earle and Shearer (1994) modified Allen's algorithm to improve the picking precision for low SNR data. Morita and Hamaguchi (1984), Sleeman and van Eck (1999) applied auto-regressive theories to pick arrivals. Picking method based on manifold has been applied to pick P-phase by two ingredients (Taylor et al., 2011). Anant and Dowla (1997), Yung and Ikelle (1997), Simons et al. (2006) applied wavelet decomposition to pick arrivals using wavelet transform as a tool. Van Decar and Crosson (1990), Ait Laasri et al. (2014) proposed arrival picking methods by cross correlation techniques, which took the first arrival by calculating cross correlation between reference seismic traces and others. Vidale (1986), Kulesh et al. (2007) picked arrivals by analyzing polarization characteristic of P- and S-wave. Wang and Teng (1995), Gentili and Michelini (2006) presented a picking method using a trained neural network, respectively. A P-phase picking method was proposed by Tselentis et al. (2012), which can adopt different picking solutions according to different situations.

However, any single method such as STA/LTA, AIC (Akaike information criterion), correlation method (Senkaya and Karsli, 2014) and others (Dai and Macbeth, 1997; Leonard and Kennett, 1999; Sheng et al., 2015; Akram et al., 2016; Kim et al., 2017) has not a good recognition effect because the low signal-to-noise ratio of microseismic signals seriously affects the accuracy of arrival picking, and even leads to a wrong picking result. Furthermore, manual picking will take a lot of time and reduce the data processing efficiency (Leonard, 2000), which cannot meet the real-time demands of microseismic data processing (Galiana-Merino et al., 2008). Therefore, how to carry out fast and precise first arrival picking is important to microseismic data processing.

Higher order statistics (HOS) is a new signal analysis and processing technology developed in recent years, it can provide high order statistical characteristics of stochastic processes (Yung and Ikelle, 1997). PAI-S/K method was proposed to pick first arrivals by Saragiotis et al. (1999, 2002, 2004), taking the Skewness and Kurtosis functions as characteristic quantity. Galiana-Merino et al. (2008) proposed a Kurtosis method to pick P-phase using the stationary wavelet technique, which efficiently provided a good estimate of the onset picks. Kuperkoch et al. (2010) combined the Akaike information criterion (AIC) with the PAI-K picking method to pick P-phase, which showed that the result was better than Allen's. Ross and Ben-Zion (2014) used HOS to identify P-waves and S-waves. Liu et al. (2014) applied the PAI-S/K method to pick arrivals on mining signal, and obtain a satisfactory picking result. Baillard et al. (2014) improved the first arrival picking precision by modifying the Kurtosis characteristic function. Sheng et al. (2015a) and Li et al. (2016) combined wavelet transform and Kurtosis function to pick first arrivals.

In recent years, shearlet transform has attracted more and more attention as a new multiscale analysis technique with better performance (Guo and Labate, 2007). Compared with curvelet transform, contourlet transform and other multiscale analysis techniques, shearlet transform has more sensitive directivity and better sparse representation performance (Kutyniok and Labate, 2009; Guo and Labate, 2010). Because of these advantages, shearlet transform has been successfully applied to many areas such as video denoising and medical images enhancement (Anju et al., 2016; Priya and Jayanthi, 2017; Cao et al., 2017; Moussa and Khelifa, 2018). In seismic data processing, it has also been widely used. Wang and Li (2013) used the shearlet and TT transforms to attenuate surface waves, which showed that the method could suppress surface waves and maintain the amplitude and phase information of reflection waves. Merouane et al. (2015) applied 2D shearlet transform to attenuation random noise. Assous and Elkington (2018) combined shearlet transform with sparse representation to imprint the downhole image, and the result showed that the method could get more accurate reconstruction of sharp high-contrast edges. Zhang (2018) applied 3D shearlet transform on microseismic data to increase the data SNR, tests show that the method can improve the weak signals to some extent.

In this paper, a P-phase picking method has been proposed based on shearlet transform and higher-order-statistics, named the S-S/L\_K (Shearlet-Short time window/Long time window-Kurtosis) method. First, we decompose the microseismic signal by shearlet transform to get the shearlet coefficients. Then, we apply the S/L\_Kur (Short time window/Long time window-Kurtosis) method on the coefficient to get first arrival time. Tests by synthetic and real data in the Shengli oil field show that the method proposed in the paper has a better and more accurate picking result than that of STA/LTA and PAI-S/K methods.

## THE PAI-S/K ALGORITHM

Saragiotis (2002) proposed a first arrival picking method based on higher order statistic, which is named Phase Arrival Identification–Skewness/Kurtosis algorithm or PAI-S/K algorithm. The skewness and Kurtosis of the series are obtained by sliding a time window on the signal. The Kurtosis and skewness can be calculated as follows (Saragiotis et al., 2002),

$$K = \frac{\sum_{i=1}^M (x_i - \bar{x})^4}{(M-1)\sigma_x^4} - 3, \quad (1)$$

$$S = \frac{\sum_{i=1}^M (x_i - \bar{x})^3}{(M-1)\sigma_x^3}, \quad (2)$$

where  $\{x_i\}$  is a discrete real number sequence with finite length  $M$ ,  $\bar{x}$  is the mean value of the series  $\{x_i\}$ ,  $\sigma_x$  is the standard deviation. The algorithm is robust and has a certain suppressing effect on Gaussian noise. Kurtosis function is more sensitive to abnormal signals compared with skewness (Tselentis et al., 2012). Therefore, the Kurtosis function is more suitable for detection of effective microseismic signals. The max value of the Kurtosis is defined as the P-phase picked by this method.

The PAI-S/K algorithm performs well for the signal with high SNR (Lokajíček and Klima, 2006; Liu et al., 2014). However, for the signal with low SNR, this algorithm cannot have an accurate result because the P-phase is hidden in noise and the max value of the kurtosis calculated by noise is greater than one calculated by effective signal (Nippres et al., 2010). Therefore, for the microseismic signal, the maximum extremal point of picking curve usually does not corresponds to the arrival position. Meanwhile, the actual microseismic data obeys generalized Gaussian distribution as a whole (Waldon, 1986). If the location of a certain underground space is fractured, the asymmetry and non-Gauss distribution characteristics of the microseismic signals within a certain fracture range are strong. Therefore, effective signals can be identified by analyzing Gauss and non-Gauss characteristics of signals. However, the effective signals hidden in noises cannot be recognized and picked up easily because of the low SNR of the microseismic data, if constant time windows are still used, local asymmetry and non-Gaussian will often be caused by noise at the same time (Hu et al., 2012). Therefore, it is necessary to improve the PAI-S/K algorithm to enhance the picking accuracy for microseismic monitoring.

In order to highlight the asymmetric and non-Gauss characteristics of local microseismic signal and overcome the problems above, we can use the idea of STA/LTA algorithm (Allen, 1978) to pick microseismic signal arrivals by sliding the long and short time window.

## METHODOLOGY

### The STA/LTA algorithm

The STA/LTA algorithm is given as follows

$$\lambda(k) = \frac{STA(k)}{LTA(k)} = \frac{\frac{1}{W_{STA}} \sum_{n=k-W_{STA}}^k |x(n)|}{\frac{1}{W_{LTA}} \sum_{n=k-W_{LTA}}^k |x(n)|}, \quad (3)$$

where  $x(n)$  is the signal time series with  $n$  sample points,  $W_{STA}$ ,  $W_{LTA}$  represents the time window width of the short time and long time window respectively (Hafez et al., 2009, 2010).

The simple structure provides a high calculation speed of STA/LTA algorithm. However, this method cannot meet the accuracy requirement for low SNR signals. Therefore, it is of great significance to improve the picking precision of microseismic signal in the situation of weak data SNR.

### The S/L\_Kur algorithm

Based on the STA/LTA algorithm and PAI-S/K algorithm, the S/L\_Kur algorithm (Sheng et al., 2015b) can be defined as follows

$$S / L - Kur(j) = \alpha(j) * \frac{STA(kurtosis)}{LTA(kurtosis)} = \alpha(j) * \frac{\frac{1}{W_{STA}} \sum_{n=j-W_{STA}}^j |kurtosis(x(n))|}{\frac{1}{W_{LTA}} \sum_{n=j-W_{LTA}}^j |kurtosis(x(n))|}, \quad (4)$$

$$\alpha(j) = \frac{\sigma_{NSTA}}{\sigma_{NLTA}}, \quad (5)$$

where  $W_{STA}$ ,  $W_{LTA}$  represents the time window width of the short time and long time window respectively.  $\sigma_{NLTA}$ ,  $\sigma_{NSTA}$  is the signal standard deviation of the short time and long time window respectively. Finally, we determine the position with the highest slope of the S/L\_Kur curve before the maximum point as the arrival point.

### *Weight factor $\alpha(j)$*

The signal standard deviation can judge the distance of the amplitude deviates from the mean value. However, microseismic effective signals are coupled with strong noises. As a consequence, the monitoring data has a low SNR in most cases, and noise has great influences on the accurate picking of microseismic signal from the beginning to the end (Hildyard et al., 2008). Before the microseismic effective signal arrived, the standard deviation of the background noise in the long and short time window has nearly the same value, so the ratio of the standard deviation in the long and short window tends to be 1. Once the microseismic event occurs and effective signal arrives, the increment of the standard deviation in the short time window is much greater than that of long time window, and the ratio of the standard deviation of the signal in the long and short window greatly increased. Therefore, weight factor  $\alpha(j)$  is introduced to increase the sensitive of the first arrival picking method.

### *Time window selection*

The selection of time window is very important for S/L\_Kur algorithm. Because this method is based on the statistical characteristics between signal and noise to pick P-wave arrivals, the length of time window should not have too much difference. First of all, the length of long time window should not be too large. If not, it can not only increase the unnecessary calculation, but also bring information redundancy to decrease the accuracy; secondly, short time window needs to be moderate. A too long or too short short-time window will cause losing statistical effects of effective signal, so that the signal cannot be effectively distinguished and identified. Therefore, in actual practice, short-time window is selected within 30-100 ms, the best difference between long and short time window is 5-10 ms (Sheng et al., 2015b).

## **Non-subsampled shearlet transform**

Shearlet transform has more sensitive directivity and better sparse representation performance, so that it can capture signal contour information more effectively. Because of its outstanding characteristics, shearlet transform (Guo and Labate, 2007) shows a good development space and prospect.

To improve the shearlet transform effect and overcome spectrum aliasing (Kong and Liu, 2013) phenomenon, Easley et al. (2008) proposed the NSST (non-subsampled shearlet transform), which mapped the standard shear wave filter from the pseudo-polarized lattice coordinate system to the Carle coordinate system. NSP (non-subsampled Laplacian pyramid) is multiscale decomposition process and SF (shearlet filter) is local directional process, which can carry out multi-directional decompose with  $l$  stages (Liang et al., 2017).

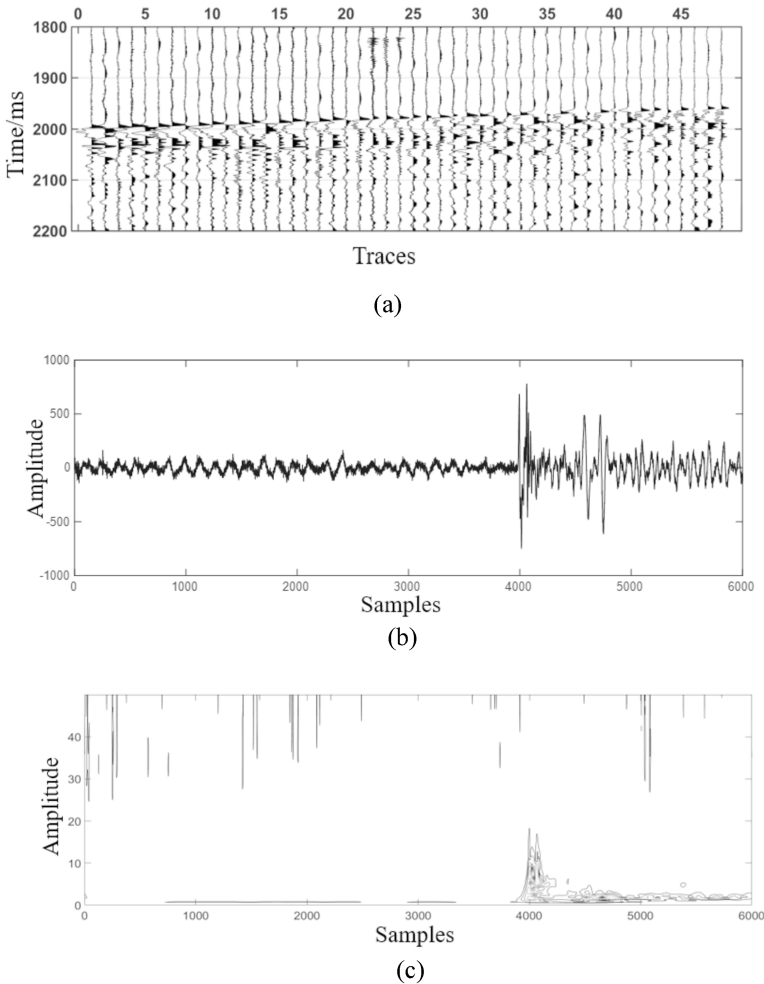


Fig. 1. A real microseismic monitoring data in the Sichuan area and its time-frequency spectrum. (a) The real microseismic data in the Sichuan area of China. (b) The first trace signal of (a). (c) The time-frequency spectrum of (b) obtained by S-transform.

Fig. 1 is a real microseismic signal in the Sichuan area and its time-frequency spectrum obtained by S-transform (Sheng et al., 2015a). From Fig. 1, we know that compared with noise, the effective microseismic signal has a lower frequency. So we can take advantage of the shearlet transform in multiscale decomposition to separate effective signals from noise and then pick the P-phase on the decomposed signal.

Based on Fig. 1, we can conclude that in order to efficiently implement the method proposed in this paper, microseismic signal energy should have a different frequency range than the noise.

## The S-S/L\_K algorithm

According to the shearlet transform and S/L\_Kur theories, the S-S/L\_K algorithm is demonstrated in Fig. 2. At the beginning, the shearlet transform is applied to decompose the microseismic data and obtain the shearlet coefficients. Then the time-frequency analysis of microseismic data such as S-transform is carried out to determine the effective signal frequency bands, so that the scales of shearlet coefficients of the effective signal can be determined. After decomposing the microseismic data by shearlet transform, the noise will be distributed in any direction, while effective signals will occur in some specific directions. Therefore, effective signals are strongly correlated in the same direction between adjacent scale layers (Cheng et al., 2017). Based on this, we can determine the directional components of shearlet coefficients where the effective signal located. Finally, by substituting the signal based on the directional components of the shearlet coefficients scale where effective signal located, the S/L\_Kur picking method is used to pick arrivals. Procedures of the S-S/L\_K algorithm are demonstrated as follows:

- (1) Processing begin: Load microseismic monitoring data  $x(n)$ .
- (2) Decomposition: Decompose the signal  $x(n)$  by shearlet transform and obtain the shearlet coefficients.
- (3) Determine the scale where effective signal located: Carry out time-frequency analysis to obtain the frequency bands of effective signals. As shown in Fig. 1, microseismic signals and noises have a certain frequency range. Since the effective signals are highly correlated within the unified monitoring range, band ranges of the effective signal frequency are roughly the same under the same observation system. Therefore, signals with high signal-to-noise ratio and good quality can be selected for time-frequency analysis such as S-transform, to obtain a rough effective signal range. Then, the approximate scale of an effective signal can be obtained according to the frequency relation corresponding to the coefficients derived from shearlet decomposition. In this way, we can avoid processing every scale and improve the processing efficiency. And then, determine the coefficient scales according to the frequency of the effective signal.
- (4) Determine the direction of the effective signal: Compute the correlation of adjacent scale layers obtained by procedure (3) under specific directions, and determine the directions according to the maximum correlation. Calculation procedure is as follows:

$$\text{Correlation}(k) = U(j, k) * U(j+1, k) \quad , \quad (6)$$

where  $U$  is the coefficients obtained by procedure (3),  $j$ ,  $k$  represents the scale and direction number, respectively (Dong et al., 2018).

- (5) Apply the S/L\_Kur picking method to pick P-phase: Substitute the signal by  $U(k)$  obtained by procedure (4) and the S/L\_Kur picking method is used to pick the P-phase.



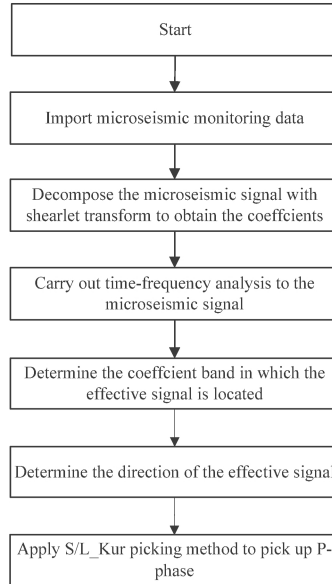


Fig. 2. The S-S/L\_K algorithm procedure.

## TESTS BY FORWARD RECORDS

### Picking results with Gaussian noise

The signal shown in Fig. 3 is obtained from forward modeling of two-dimensional staggered grid finite difference wave equation. The main frequency of the signal is 20 Hz, and the source depth is 1600 m.

It is well known that SNR has great influence on the accuracy of P-phase picking. Therefore, Gaussian noise with SNR=-1 dB (Fig. 4), -5 dB (Fig.7), -10 dB (Fig. 9) and -20 dB (Fig. 11) was added to the signal respectively to test the validity of the algorithm. Fig. 6, Fig. 8, Fig. 10 and Fig. 12 is the picking result by S-S/L\_K algorithm, PAI-K algorithm and STA/LTA algorithm corresponding to Fig. 4, Fig. 7, Fig. 9, and Fig. 11, respectively. The SNR in this paper is defined as follows

$$S / N = 10 \log_{10} \left( \frac{\sigma_s}{\sigma_n} \right) \quad (7)$$

where  $\sigma_s, \sigma_n$  represents the standard deviation of the original signal and the added noise respectively. Shearlet transform with scale 5 is used to decompose the simulated microseismic signal. The coefficient structure of shearlet transform is shown in Table 1.

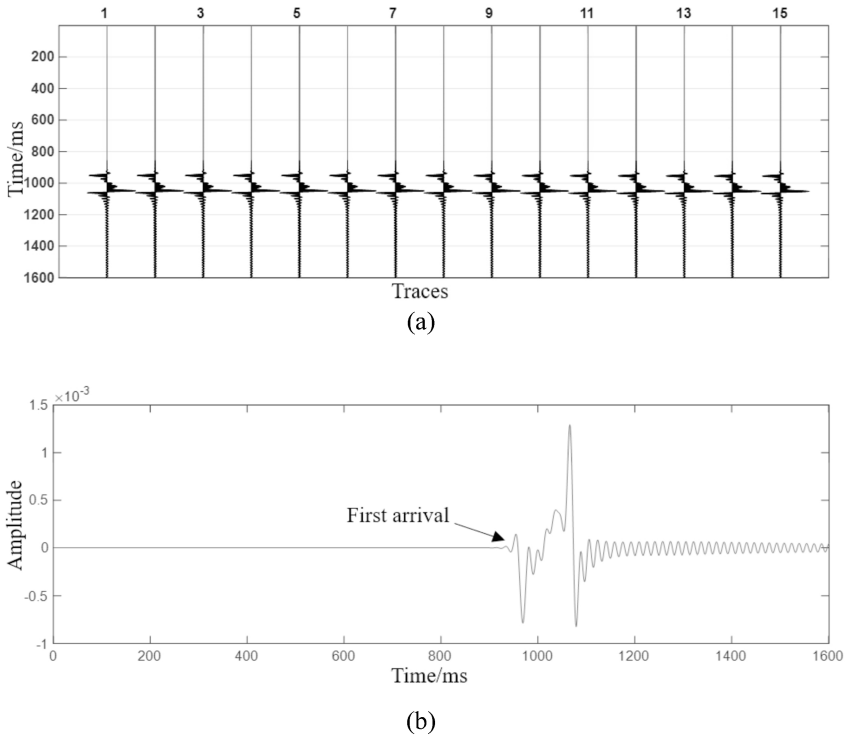
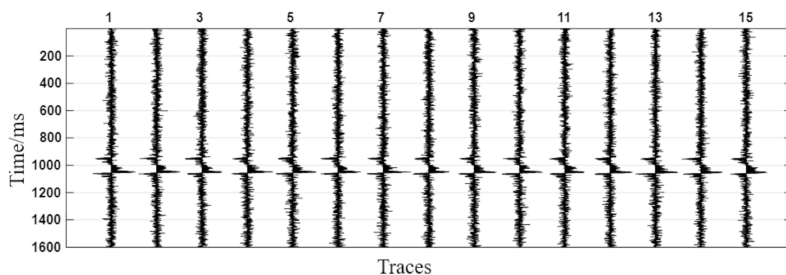


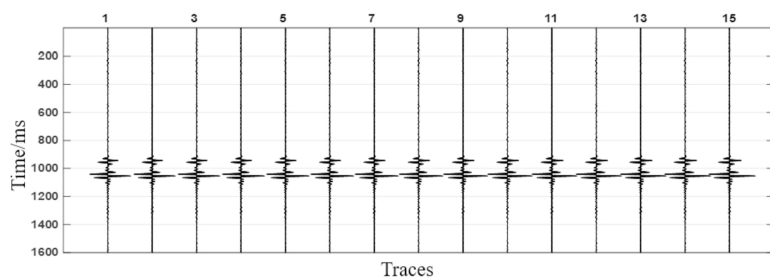
Fig. 3. Forward modeling signal with arrival time 940 ms. (a) Modeling forward record. (b) The 1st trace of (a).

Table 1. Coefficient structure of shearlet transform.

Layer	Scale	Direction number
Coarse	C{1}	1
	C{2}	6
Detail	C{3}	6
	C{4}	10
Fine	C{5}	10

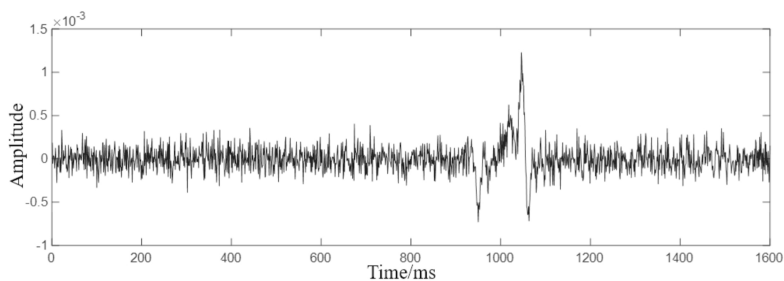


(a)

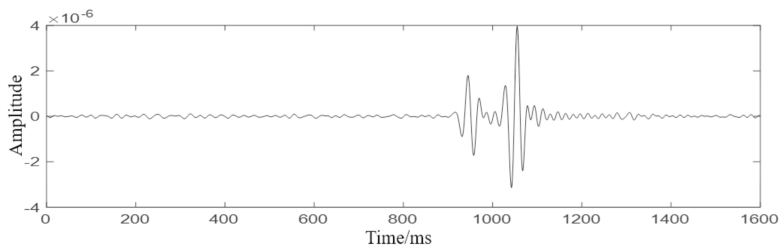


(b)

Fig. 4. Forward modeling signal with SNR = -1 dB and the signal after decomposing. (a) Modeling forward record. (b) Signal after decomposing.

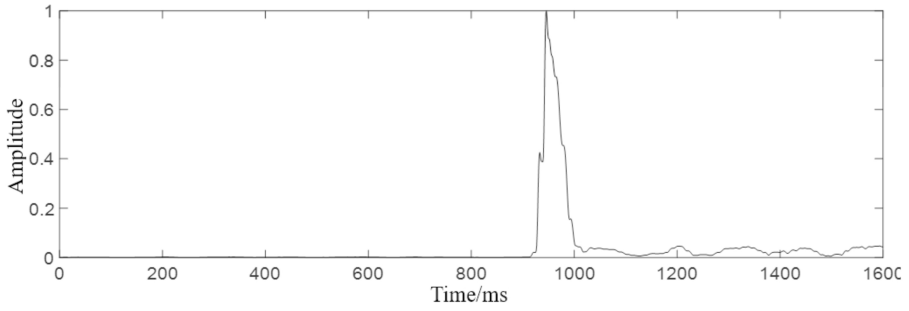


(a)

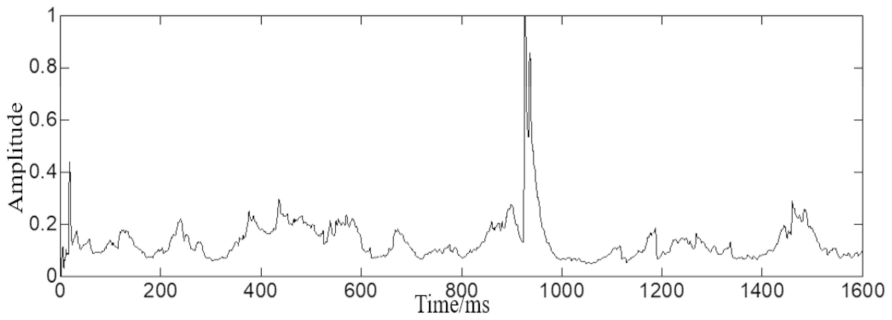


(b)

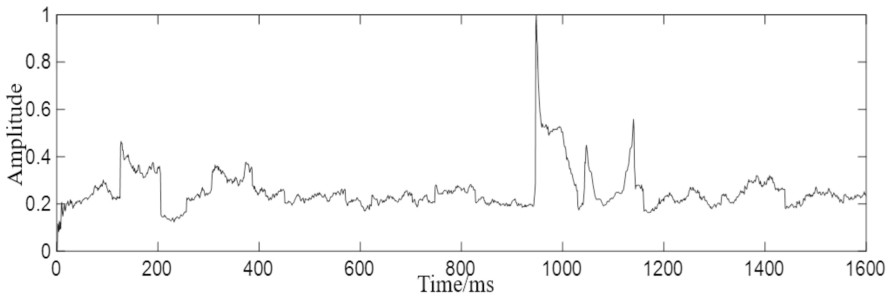
Fig. 5. Shearlet decomposing details of the 1st trace of Fig. 4(a). (a) The 1st trace of Fig.4(a). (b) Signal of (a) after decomposing.



(a)

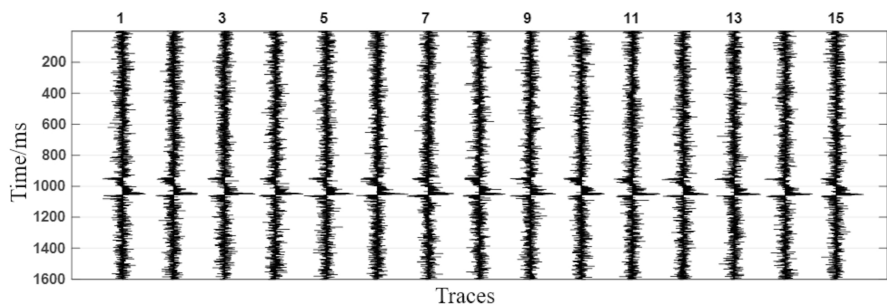


(b)

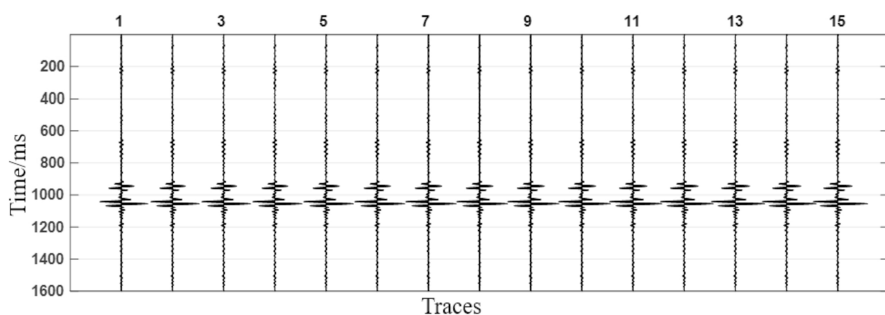


(c)

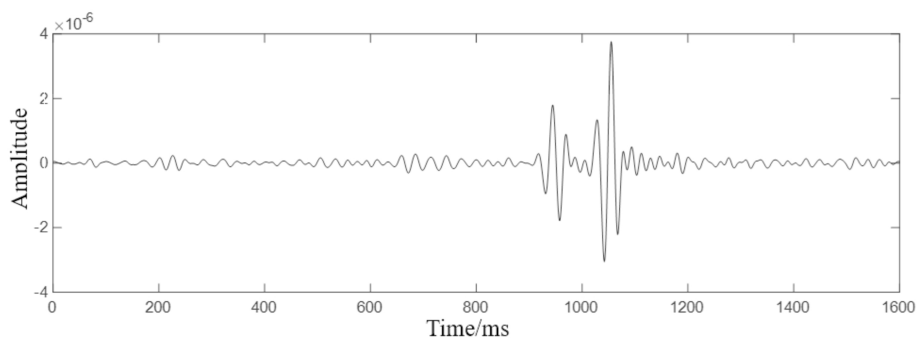
Fig. 6. Picking curve of the 1st trace of Fig. 4(a) by S-S/L\_K algorithm, PAI-K algorithm and STA/LTA algorithm. (a) Picking curve by S-S/L\_K algorithm. (b) Picking curve by PAI-K algorithm. (c) Picking curve by STA/LTA algorithm.



(a)

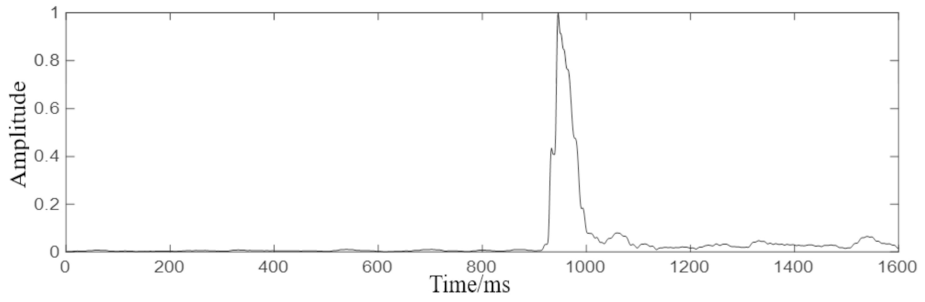


(b)

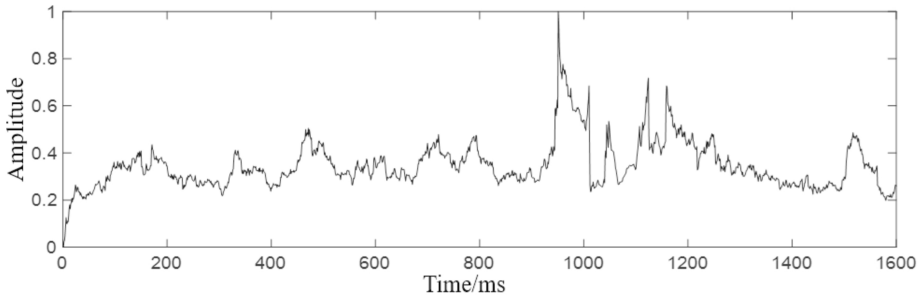


(c)

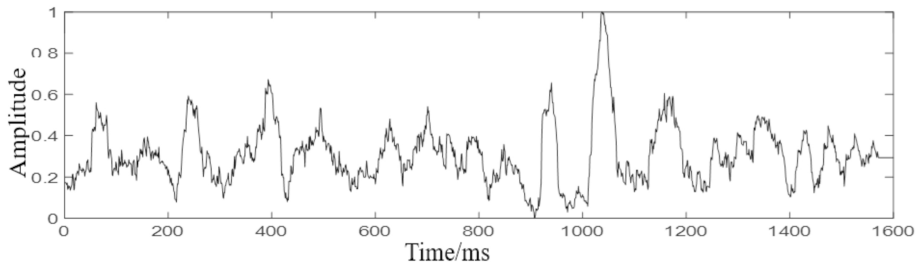
Fig. 7. Forward modeling signal with SNR = -5 dB and the signal after decomposing. (a) Modeling forward record. (b) Signal after decomposing. (c) The 1st trace of (b).



(a)

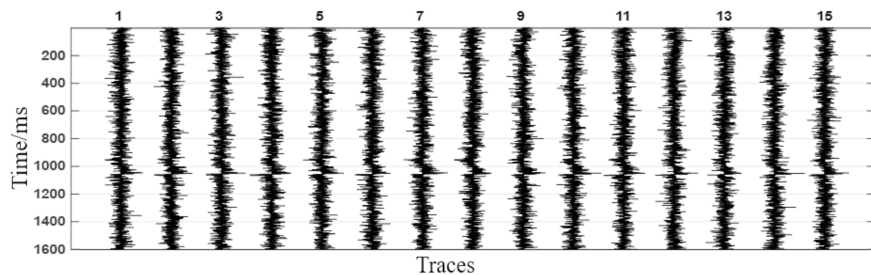


(b)

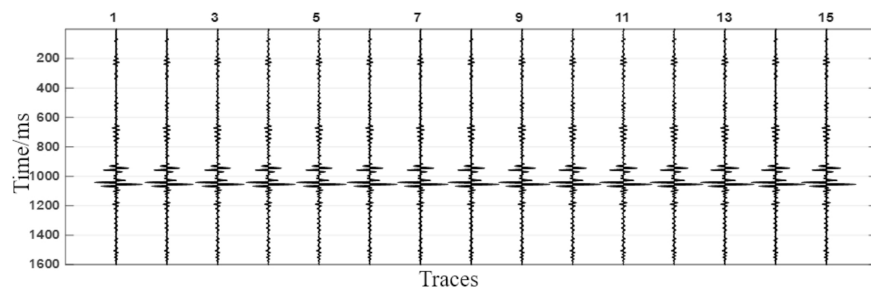


(c)

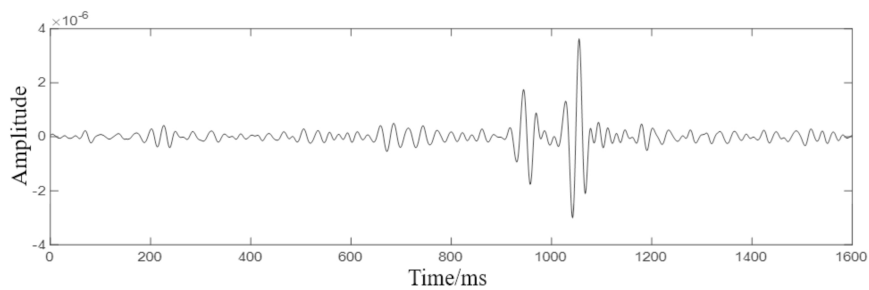
Fig. 8. Picking curve of the 1<sup>st</sup> trace of fig.7 (a) by S-S/L\_K algorithm, PAI-K algorithm and STA/LTA algorithm. (a) Picking curve by S-S/L\_K algorithm. (b) Picking curve by PAI-K algorithm. (c) Picking curve by STA/LTA algorithm.



(a)

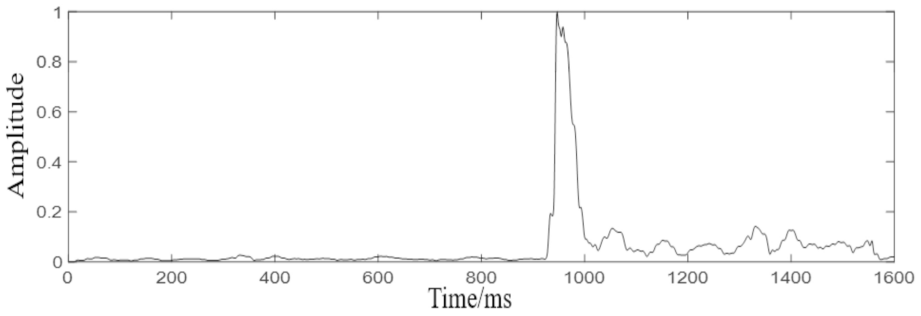


(b)

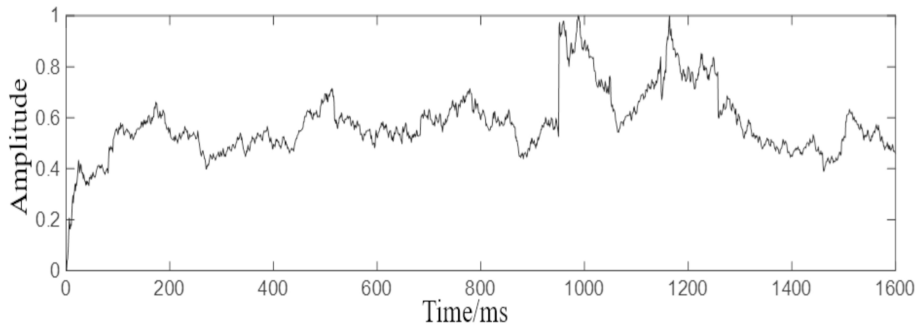


(c)

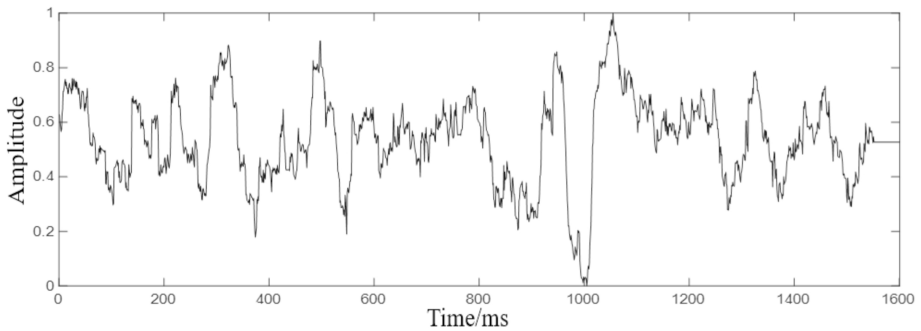
Fig. 9. Forward modeling signal with SNR = -10 dB and the signal after decomposing. (a) Modeling forward record. (b) Signal after decomposing. (c) The 1st trace of (b).



(a)



(b)



(c)

Fig. 10. Picking curve of the 1st trace of Fig. 9(a) by S-S/L\_K algorithm, PAI-K algorithm and STA/LTA algorithm. (a) Picking curve by S-S/L\_K algorithm. (b) Picking curve by PAI-K algorithm. (c) Picking curve by STA/LTA algorithm.



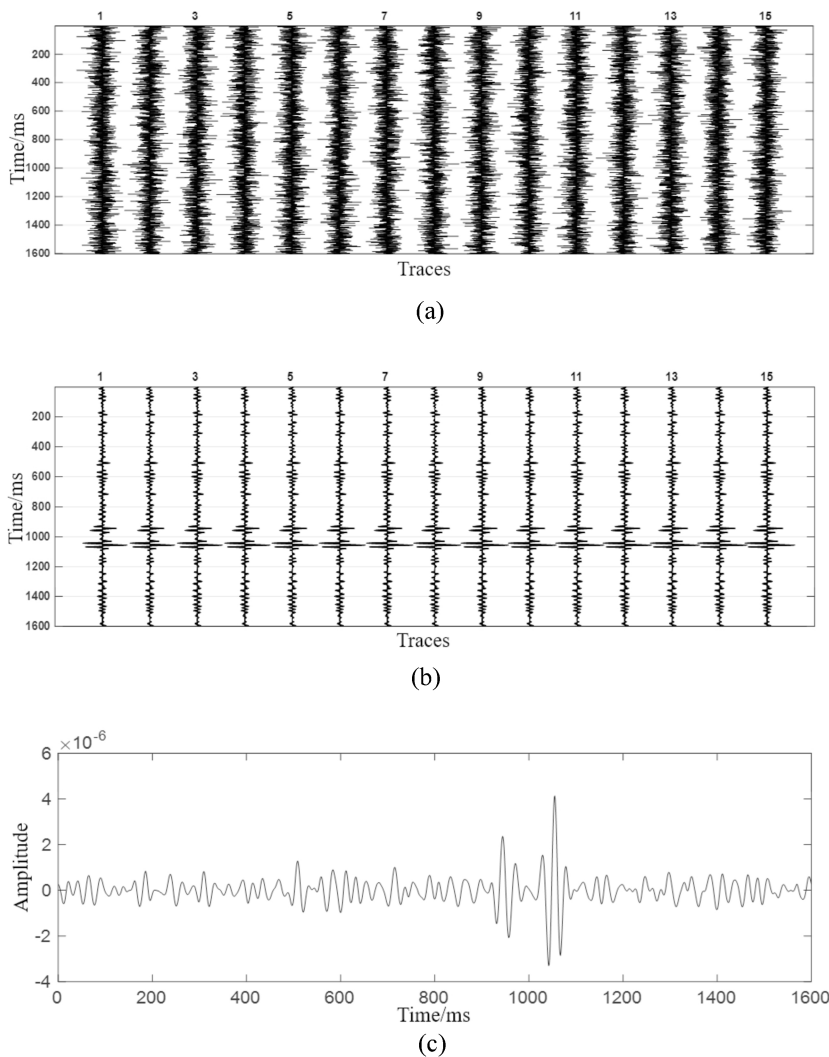


Fig. 11. Forward modeling signal with SNR = -20 dB and the signal after decomposing. (a) Modeling forward record. (b) Signal after decomposing. (c) The 1st trace of (b).

From Fig. 6, Fig. 8, Fig. 10 and Fig. 12, we can conclude that the PAI-K algorithm and STA/LTA algorithm obtain obvious wrong results for the signal with SNR from -5 dB to -20 dB. Compared with the two algorithms mentioned earlier, the picking curve of the S-S/L\_K algorithm is not only much smoother but also jumps more clearly, especially has higher accuracy even for the signal with a poor SNR.

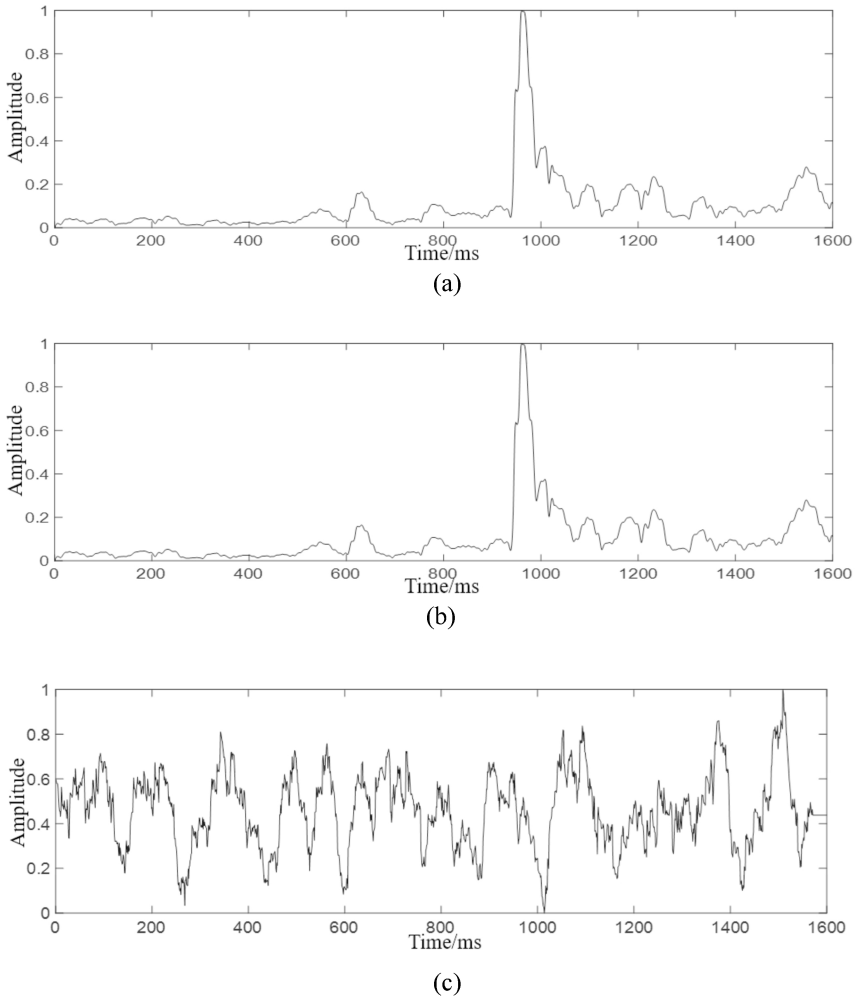
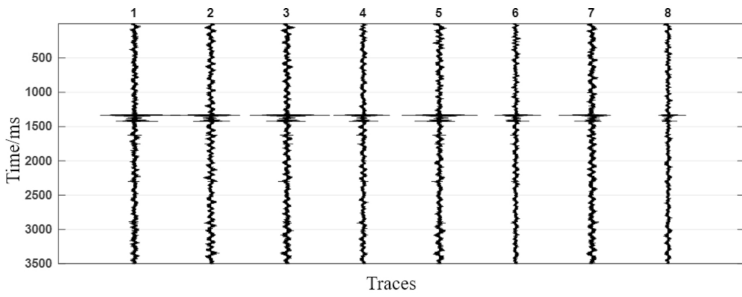


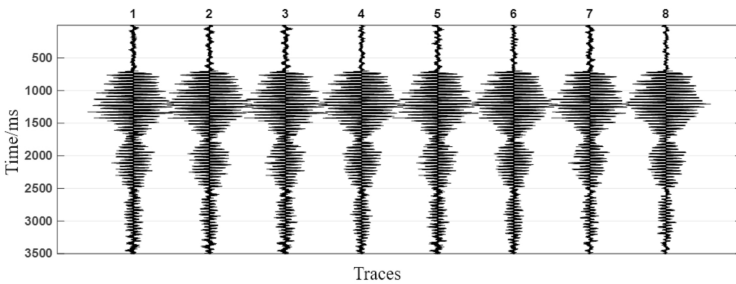
Fig. 12. Picking curve of the 1st trace of Fig. 11(a) by S-S/L\_K algorithm, PAI-K algorithm and STA/LTA algorithm. (a) Picking curve by S-S/L\_K algorithm. (b) Picking curve by PAI-K algorithm. (c) Picking curve by STA/LTA algorithm.

### Picking results with correlated noise

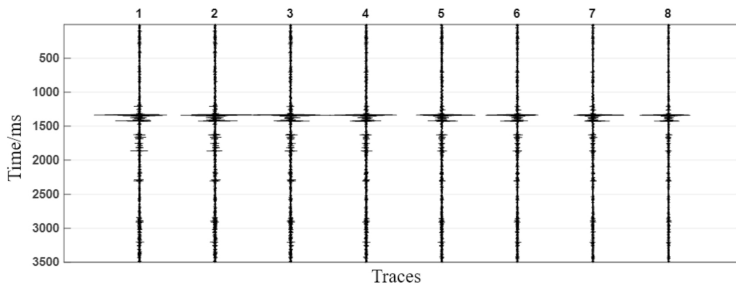
Fig. 13(a) is a real microseismic monitoring data with a total of 8 receivers in Shengli oil field. Every signal length is 3500 ms and the sample interval is 1 ms. Then, the noises separated from another set of real monitoring data are added to every signal of Fig. 13(a) to test the application effect of the algorithm in the presence of strong correlated noises. Fig. 13 is the shearlet decomposing details of the signal. And Fig. 14 is the picking result by S-S/L\_K algorithm, PAI-K algorithm and STA/LTA algorithm corresponding to Fig. 13, respectively.



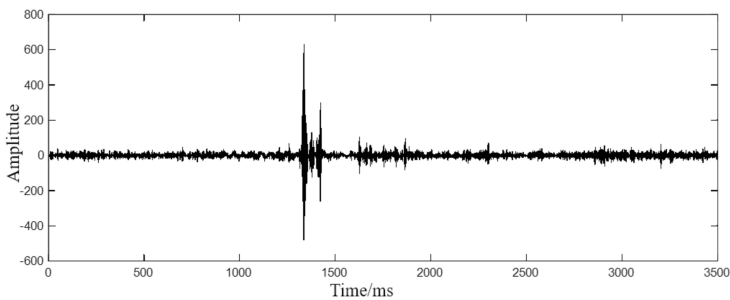
(a)



(b)

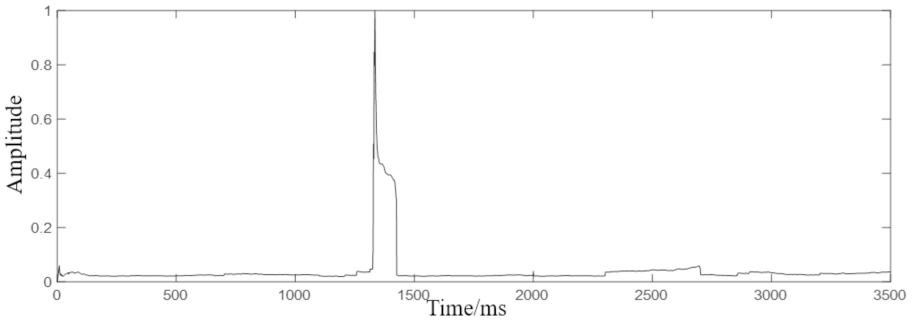


(c)

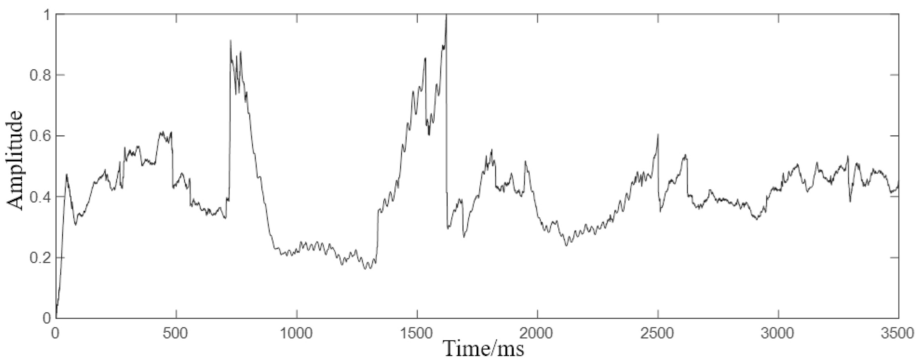


(d)

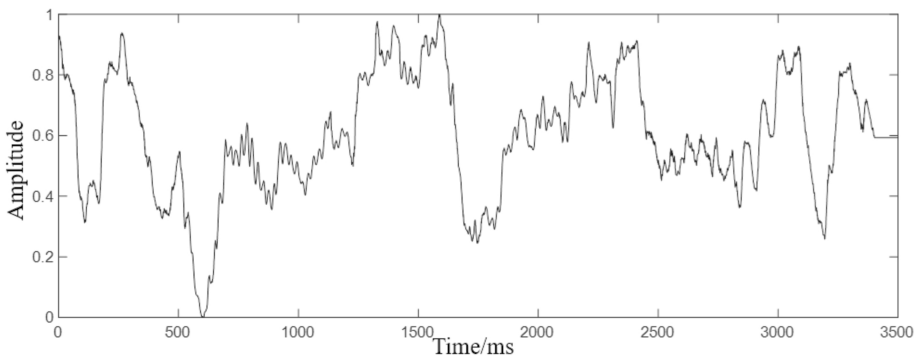
Fig. 13. Shearlet decomposing details of the 5th trace of Fig. 13(b). (a) Real monitoring data in the Shengli oil field. (b) Real monitoring data added with correlated noise. (c) The signal after decomposing. (d) The 5th trace signal of Fig.13(c) after decomposing.



(a)



(b)



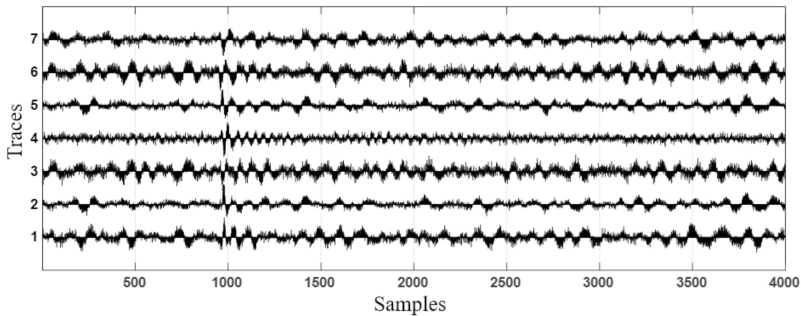
(c)

Fig. 14. Picking curve of the signal of Fig. 13(d) by S-S/L\_K algorithm, PAI-K algorithm and STA/LTA algorithm. (a) Picking curve by S-S/L\_K algorithm. (b) Picking curve by PAI-K algorithm. (c) Picking curve by STA/LTA algorithm.

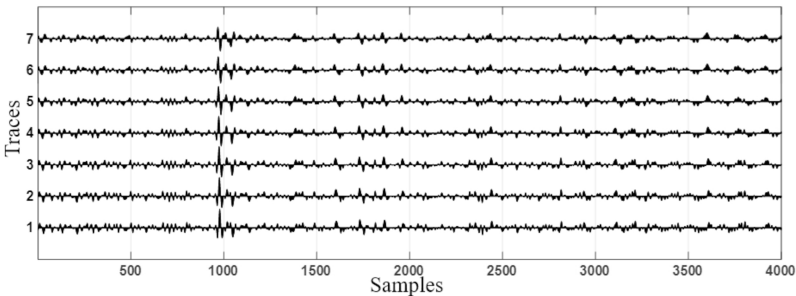
From Fig. 14, we can see that compared with the S-S/L\_K algorithm, both of the other algorithms obtain obviously wrong picking results while the S-S/L\_K algorithm still has reliable picking accuracy in the presence of strong correlated noises.

## REAL DATA PROCESSING

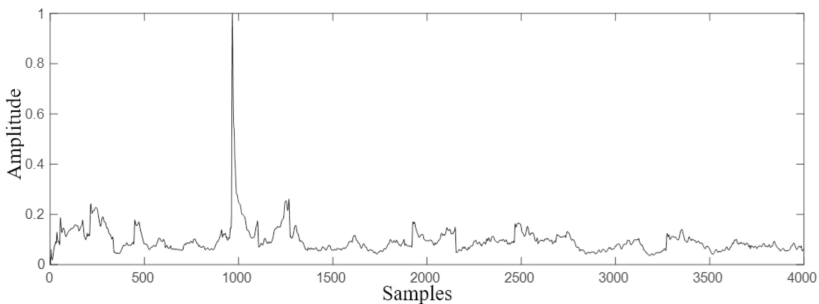
Fig. 15 is a real microseismic monitoring data with a total of 7 receivers in the Shengli oil field. Every signal length is 2000 ms and the sample interval is 0.5 ms. The S-S/L\_K algorithm is applied on this data to test the application effect of the algorithm in actual practice, meanwhile the STA/LTA algorithm is used for comparison.



(a)



(b)



(c)

Fig. 15. Picking result of real data in the Shengli oil field by S-S/L\_K algorithm and STA/LTA algorithm. (a) Real monitoring data in the Shengli oil field. (b) The signal of Fig. 15(a) after decomposing. (c) Picking curve of the 1st trace of Fig. 15(a) by S-S/L\_K algorithm.

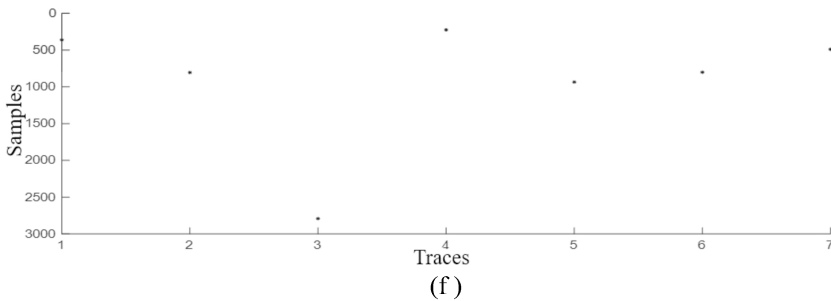
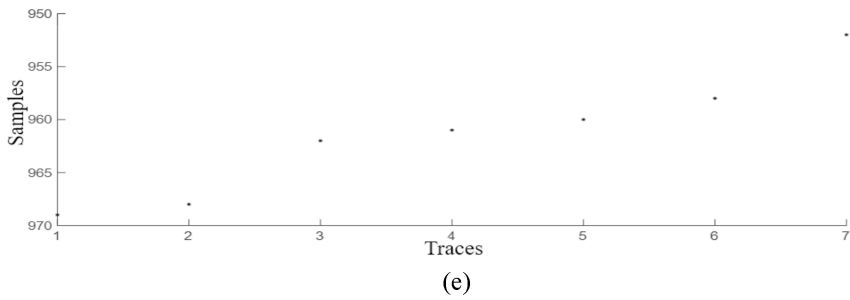
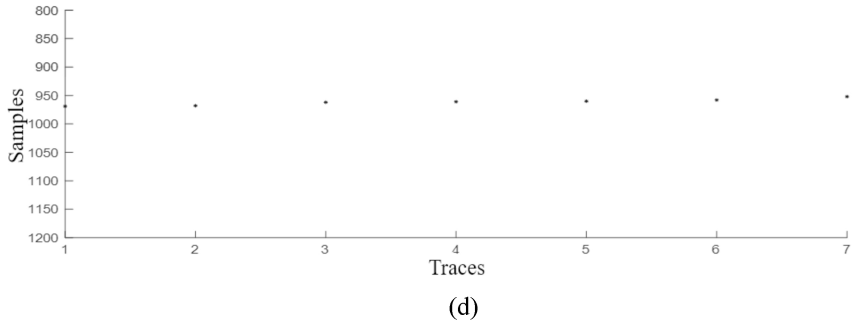


Fig. 15. Picking result of real data in the Shengli oil field by S-S/L\_K algorithm and STA/LTA algorithm. (d) Picking result of all traces by S-S/L\_K algorithm. (e) Magnification of picking result shown in (c). (f) Picking result of all traces by STA/LTA algorithm.

From Fig. 15, we can see that the picking result by S-S/L\_K algorithm is very accurate and fits very well with the real monitoring data. The final picking sample almost distributed between 952 and 968. However, compared with the S-S/L\_K algorithm, the STA/LTA algorithm has a poor picking result with a picking sample distribution between 480-2800.

## CONCLUSION

In this paper, we have developed the PAI-S/K algorithm and combined the shearlet multiscale decomposition with HOS, and finally formed the S-S/L\_K algorithm. In order to verify the algorithm presented in this paper, lots of tests have been carried out. First, Gaussian noise with SNR = -1 dB, -5 dB, -10 dB and -20 dB was added to the forward modeling signal, respectively, to test the validity of the algorithm, and then, in order to better simulate the actual situation, a group of correlated noises was added. Meanwhile the PAI-K and STA/LTA algorithms are used for comparison. Tests by forward modeling signal show that compared with the PAI-K and STA/LTA picking methods, the S-S/L\_K algorithm can obtain a more accurate and satisfactory result. This algorithm not only keeps the advantage of non-subsampled shearlet transform in multiscale analysis, but also keeps the advantage of HOS in signal anomalies detection and Gaussian noise suppressing. Finally, the S-S/L\_K algorithm was applied to real microseismic monitoring data in the Shengli oil field, with the STA/LTA picking result for comparison. The synthetic examples and real data tests show that our proposed method can overcome the influence of noise on the P-phase picking accuracy and obtain a reliable P-phase result for microseismic monitoring.

## ACKNOWLEDGMENTS

This research is financially supported by the National Natural Science Foundation of China (41674107) and the National Key Research and Development Program of China under Grant 2017YFB0202904, Youth Fund of Yangtze University (2016CQN10) and Open Fund of Key Laboratory of Exploration Technologies for Oil and Gas Resources (Yangtze University), Ministry of Education, No. K2018-15.

## REFERENCES

- Ait Laasri, E.H., Akhouayri, E.-S., Agliz, D. and Atmani, A., 2014. Automatic detection and picking of P-wave arrival in locally stationary noise using cross-correlation. *Digit. Sign. Process.*, 26: 87-100.
- Akram, J. and Eaton, D.W., 2016. A review and appraisal of arrival-time picking methods for downhole microseismic data. *Geophysics*, 81(2): KS67-KS87.
- Allen, R.V., 1978. Automatic earthquake recognition and timing from single traces. *Bull. Seismol. Soc. Am.*, 68; 1521-1532.
- Alvarez, I., Garcia, L., Mota, S., Cortes, G., Benitez, C. and de la Torre, A., 2013. An automatic P-phase picking algorithm based on adaptive multiband processing. *IEEE Geosci. Remote Sens. Lett.*, 10: 1488-1492.  
<http://dx.doi.org/10.1109/LGRS.2013.2260720>.
- Anant, K.S. and Dowla, F.U., 1997. Wavelet transform methods for phase identification in three-component seismograms. *Bull. Seismol. Soc. Am.*, 87: 1598-1612.
- Anju, T.S. and Raj, N.R.N., 2016. Shearlet transform based image denoising using histogram thresholding. *Internat. Conf. Communicat. Syst. Netw. (ComNet)*: 162-166.

- Assous, A. and Elkington, P., 2018. Shearlets and sparse representation for micro-resistivity borehole image inpainting. *Geophysics*, 83(1): D17-D25.
- Baillard, C., Crawford, W.C., Ballu, V., Hibert, C. and Mangeney, A., 2014. An automatic Kurtosis based P-and S-phase picker designed for local seismic networks. *Bull. Seismol. Soc. Am.*, 104: 394-409. <http://dx.doi.org/10.1785/0120120347>.
- Cao, Q., Li, B. and Fan, L., 2017. Medical image fusion based on GPU accelerated non-subsampled shearlet transform and 2D principal component analysis. *IEEE 2nd Internat. Conf. Sign. Image Process. (ICSIP)*: 203-207. doi: 10.1109/SIPROCESS.2017.8124533
- Cheng, Y., Li, Y. and Zhang, C., 2017. First arrival time picking for microseismic data based on shearlet transform. *J. Geophys. Engineer.*, 14: 262-271.
- Dai, H. and Macbeth, C., 1997. The application of back-propagation neural network to automatic picking seismic arrivals from single-component recordings. *J. Geophys. Res.-Solid Earth*, 102(B7): 15105-15113.
- Dong, L.J., Wesseloo, J., Potvin, Y. and Li, X.B., 2016. Discrimination of mine seismic events and blasts using the Fisher classifier, naive Bayesian classifier and logistic regression. *Rock Mechan. Rock Engineer.*, 49: 183-211. <https://doi.org/10.1007/s00603-015-0733-y>.
- Dong, X., Li, Y., Wu, N., Tian, Y. and Yu, P., 2018. The S-STK/LTK algorithm for arrival time picking of microseismic signals. *J. Geophys. Engineer.*, 15. doi: 10.1088/1742-2140/aab30c.
- Duncan, P.M. and Eisner, L., 2010. Reservoir characterization using surface micro-seismic monitoring. *Geophysics*, 75(3): A139-A146.
- Earle, P.S. and Shearer, P.M., 1994. Characterization of global seismograms using an automatic-picking algorithm. *Bull. Seismol. Soc. Am.*, 84: 366-376.
- Easley, G., Labate, D. and Lim, W.Q., 2008. Sparse directional image representations using the discrete shearlet transform. *Appl. Computat. Harmon. Analys.*, 25: 25-46.
- Galiana-Merino, J.J., Rosa-Herranz, J.L. and Parolai, S., 2008. Seismic P-phase picking using a Kurtosis-based criterion in the stationary wavelet domain. *IEEE Transact. Geosci. Remote Sens.*, 46: 3815-3826. <http://dx.doi.org/10.1109/TGRS.2008.2002647>.
- Gentili, S. and Michelini, A., 2006. Automatic picking of P- and S-phases using a neural tree. *J. Seismol.*, 10: 39-63. <http://dx.doi.org/10.1007/s10950-006-2296-6>.
- Gibbons, S.J. and Ringdal, F., 2006. The detection of low magnitude seismic events using array-based waveform correlation. *Geophys. J. Internat.*, 165: 149-166. <http://dx.doi.org/10.1111/j.1365-246X.2006.02865.x>
- Gou, X.T., Li, Z.M., Qin, N. and Jin, W.D., 2011. Adaptive picking of microseismic event arrival using a power spectrum envelope. *Comput. Geosci.*, 37: 158-164. <http://dx.doi.org/10.1016/j.cageo.2010.05.022>.
- Guo, K. and Labate, D., 2007. Optimally sparse multidimensional representations using shearlets. *SIAM J. Mathemat. Analys.*, 39: 298-318.
- Guo, K. and Labate, D., 2010. Optimally sparse 3D approximations using shearlet representations. *Electron. Res. Announcem. Mathemat. Sci.*, 17: 125-137. doi: 10.3934/era.
- Hafez, A.G., Khan, M.T.A. and Kohda, T., 2009. Earthquake onset detection using spectro-ratio on multi-threshold time-frequency sub-band. *Digit. Sign Process.*, 19: 118-126. <http://dx.doi.org/10.1016/j.dsp.2008.08.003>.
- Hafez, A.G., Khan, M.T.A. and Kohda, T., 2010. Clear P-wave arrival of weak events and automatic onset determination using wavelet filter banks. *Digit. Sign. Process.*, 20: 715-723. <http://dx.doi.org/10.1016/j.dsp.2009.10.002>.
- Hafez, A.G., Rabie, M. and Kohda, T., 2013. Seismic noise study for accurate P-wave arrival detection via MODWT. *Comput. Geosci.*, 54: 148-159. <http://dx.doi.org/10.1016/j.cageo.2012.12.002>.
- Hildyard, M.W., Nippres, S.E. and Rietbrock, A., 2008. Event detection and phase picking using a time-domain estimate of predominate period Tpd. *Bull. Seismol. Soc. Am.*, 98: 3025-3032. <http://dx.doi.org/10.1785/0120070272>.



- Hu, Y.Q., Yin, C., Pan, S., Wu, F., Li, Y. and Liu, Y., 2012. A microseismic signal recognition technique based on improved time-varying skewness and Kurtosis method. *Geophys. Prosp. Petrol.*, 51: 625-632.
- Kim, D., Byun, J.M., Lee, M., Choi, J. and Kim, M.S., 2017. Fast first arrival picking algorithm for noisy microseismic data. *Explor. Geophys.*, 48: 131-136.
- Küperkoch, L., Meier, T., Lee, J. and Friederich, W., 2010. Automated determination of P-phase arrival times at regional and local distances using higher order statistics. *Geophys. J. Internat.*, 181: 1159-1170.  
<http://dx.doi.org/10.1111/j.1365-246X.2010.04570.x>.
- Kutyniok, G. and Labate, D., 2009. Resolution of the wavefront set using continuous shearlets. *Transact. Am. Mathemat. Soc.*, 361: 2719-2754.
- Karamzadeh, N., Doloei, G.J. and Reza, A.M., 2013. Automatic earthquake signal onset picking based on the continuous wavelet transform. *IEEE Transact. Geosci. Remote Sens.*, 51: 2666-2674. <http://dx.doi.org/10.1109/TGRS.2012.2213824>.
- Kulesh, M., Diallo, M.S., Holschneider, M., Kurennaya, K., Kruger, F., Ohrnberger, M. and Scherbaum, E., 2007. Polarization analysis in the wavelet domain based on the adaptive covariance method. *Geophys. J. Internat.*, 170: 667-678.  
<http://dx.doi.org/10.1111/j.1365-246X.2007.03417.x>.
- Kutyniok, G. and Labate, D. 2009. Resolution of the wavefront set using continuous shearlets. *Transact. Am. Mathemat. Soc.*, 361: 2719-2754.
- Leonard, M. and Kennett, B.L.N., 1999. Multi-component autoregressive techniques for the analysis of seismograms. *Phys. Earth Planet. Inter.*, 113: 247-263.  
[http://dx.doi.org/10.1016/S0031-9201\(99\)00054-0](http://dx.doi.org/10.1016/S0031-9201(99)00054-0).
- Leonard, M., 2000. Comparison of manual and automatic onset time picking. *Bull. Seismol. Soc. Am.*, 90: 1384-1390. doi: 10.1785/0120000026.
- Li, X., Shang, X., Wang, Z., Dong, L. and Weng, L., 2016. Identifying P-phase arrivals with noise: an improved Kurtosis method based on DWT and STA/LTA. *J. Appl. Geophys.*, 133: 50-61.
- Liang, X., Li, Y. and Zhang, C., 2017. Noise suppression for microseismic data by non-subsampled shearlet transform based on singular value decomposition. *Geophys. Prosp.*, 66: 894-903. doi: 10.1111/1365-2478.12576
- Liu, J.-S., Wang, Y. and Yao, Z.-X., 2013. On micro-seismic first arrival identification: A case study. *Chin. J. Geophys.*, 56: 1660-1666.
- Liu, X.Q., Cai, Y., Zhao, R., Zhao, Y.G., Qu, B.A., Feng, Z.J. and Li, H., 2014. An automatic seismic signal detection method based on fourth-order statistics and applications. *Appl. Geophys.*, 11: 128-138.  
<http://dx.doi.org/10.1007/s11770-014-0433-5>.
- Lokajićek, T. and Klima, K., 2006. A first arrival identification system of acoustic emission (AE) signals by means of a high-order statistics approach. *Meas. Sci. Technol.*, 17: 2461. <http://dx.doi.org/10.1088/0957-0233/17/9/013>.
- Maxwell, S.C., Rutledge, J., Jones, R. and Fehler, M., 2010. Petroleum reservoir characterization using downhole microseismic monitoring. *Geophysics*, 75: A129-A137.
- Maeda, N., 1985. A method for reading and checking phase times in auto-processing system of seismic wave data. *Zisin*, 38: 365-379.
- Merouane, A., Yilmaz, O. and Baysal, E., 2015. Random noise attenuation using 2-Dimensional shearlet transform. *Expanded Abstr.*, 85th Ann. Internat. SEG Mtg., New Orleans: 4770-4774.
- Morita, Y. and Hamaguchi, H., 1984. Automatic detection of onset time of seismic waves and its confidence interval using autoregressive model fitting. *Zisin*, 37: 281-293.
- Moussa, O. and Khelifa, N., 2018. Video speckle noise reduction using robust diffusion tensor in shearlet domain. *4th Internat. Conf. Adv. Technolog. Sign. Image Process. (ATSIP)*: 1-6. doi: 10.1109/ATSIP.2018.8364523
- Nippress, S., Rietbrock, A. and Heath, A., 2010. Optimized automatic pickers: application to the ANCORP data set. *Geophys. J. Internat.*, 181: 911-925.  
<http://dx.doi.org/10.1111/j.1365-246X.2010.04531.x>.

- Priya, B.L. and Jayanthi, K., 2017. Edge enhancement of liver CT images using non subsampled shearlet transform based multislice fusion. *Internat. Conf. Wireless Communicat., Sign. Process. Network. (WiSPNET)*: 191-195.
- Ross, Z.E. and Ben-Zion, Y., 2014. Automatic picking of direct P-, S-seismic phases and fault zone head waves. *Geophys. J. Internat.*, 199: 368-381. <http://dx.doi.org/10.1093/gji/ggu267>, doi: 10.1109/CSN.2016.7824007.
- Saragiotis, C.D., Hadjileontiadis, L.J. and Panas, S.M., 1999. A higher-order statistics-based phase identification of three-component seismograms in a redundant wavelet transform domain. *Proc. IEEE Worksh. Higher Order Statist.*: 396-399.
- Saragiotis, C.D., Hadjileontiadis, L.J. and Panas, S.M., 2002. PAI-S/K: A robust automatic seismic P-phase arrival identification scheme. *IEEE Transact. Geosci. Remote Sens.*, 40: 1395-1404. <http://dx.doi.org/10.1109/TGRS.2002.800438>.
- Saragiotis, C.D., Hadjileontiadis, L.J., Rekanos, I.T. and Panas, S.M., 2004. Automatic P-phase picking using maximum Kurtosis and K-statistics criteria. *IEEE Geosci. Remote Sens. Lett.*, 1: 147-151. <http://dx.doi.org/10.1109/LGRS.2004.828915>.
- Senkaya, M. and Karli, H., 2014. A semi-automatic approach to identify first arrival time: the cross correlation technique (CCT). *Earth Sci. Res. J.*, 18: 107-113. <http://dx.doi.org/10.15446/esrj.v18n2.35887>.
- Shang, X., Li, X., Morales-Esteban, A. and Dong, L., 2018. An improved P-phase arrival picking method S/L-K-A with an application to the Yongshaba Mine in China. *Pure Appl. Geophys.*, 3: 1-19.
- Sheng, G., Li, Z. and Wang, W., 2015a. A new automatic detection method of microseismic event based on CWT and HOS. *Expanded Abstr., 85th Ann. Internat. SEG Mtg., New Orleans*: 2625-2629.
- Sheng, G., Li, Z. and Wang, W., 2015b. A new automatic detection method of microseismic events based on wavelet decomposition and high-order statistics. *Geophys. Prosp. Petrol.*, 8: 388-395.
- Sleeman, R., van Eck, T., 1999. Robust automatic P-phase picking: an on-line implementation in the analysis of broadband seismogram recordings. *Phys. Earth Planet. Inter.*, 113: 265-275. [http://dx.doi.org/10.1016/S0031-9201\(99\)00007-2](http://dx.doi.org/10.1016/S0031-9201(99)00007-2).
- Taylor, K.M., Procopio, M.J., Young, C.J. and Meyer, F.G., 2011. Estimation of arrival times from seismic waves: a manifold-based approach. *Geophys. J. Internat.*, 185: 435-452. <http://dx.doi.org/10.1111/j.1365-246X.2011.04947.x>.
- Tselentis, G.A., Martakis, N., Paraskevopoulos, P., Lois, A. and Sokos, E., 2012. Strategy for automated analysis of passive microseismic data based on S-transform, Otsu's thresholding, and higher order statistics. *Geophysics*, 77: Ks43-Ks54. <http://dx.doi.org/10.1190/geo2011-0301.1>.
- Van Decar, J. and Crosson, R., 1990. Determination of teleseismic relative phase arrival times using multi-channel cross-correlation and least squares. *Bull. Seismol. Soc. Am.*, 80: 150-169.
- Vidale, J.E., 1986. Complex polarization analysis of particle motion. *Bull. Seismol. Soc. Am.*, 76: 1393-1405.
- Walden, T. and Hosken, J.W.J., 1986. The nature of the non-Gaussianity of primary reflection coefficients and its significance for deconvolution. *Geophys. Prosp.*, 34: 1038-1066.
- Wang, J. and Teng, T.-L., 1995. Artificial neural network-based seismic detector. *Bull. Seismol. Soc. Am.*, 85: 308-319.
- Wang, D. and Li, Z.C., 2013. Surface wave attenuation using the Shearlet and TT transforms. *Expanded Abstr., 83rd Ann. Internat. SEG Mtg., Houston*: 4335-4339.
- Yung, S.K. and Ikelle, L.T., 1997. An example of seismic time picking by 3rd order bicoherence. *Geophysics*, 62: 1947-1952.
- Zhang, C. and van der Baan, M., 2018. Multicomponent microseismic data denoising by 3D shearlet transform. *Geophysics*, 83(3): A45-A51.
- Zhao, Y. and Takano, K., 1999. An artificial neural network approach for broadband seismic phase picking. *Bull. Seismol. Soc. Am.*, 89: 670-680.